Correlates of figure-ground segregation in fMRI

G. Skiera [a], D. Petersen [b], M. Skalej [b], M. Fahle [a,c,*]

[a] *Human-Neurobiology, University of Bremen, Argonnenstrasse 3, D28211 Bremen, Germany*
[b] *Department of Neuroradiology, University of Tübingen, Hoppe-Seyler-Str. 3, D-72076, Tübingen, Germany*
[c] *Department of Optometry and Visual Science, City University, 311-321 Goswell Road, London EC1V 7DD, UK*

Abstract

We investigated which correlates of figure-ground-segregation can be detected by means of functional magnetic resonance imaging (fMRI). Five subjects were scanned with a Siemens Vision 1.5 T system. Motion, colour, and luminance-defined checkerboards were presented with alternating control conditions containing one of the two features of the checkerboard. We find a segregation-specific activation in V1 for all subjects and all stimuli and conclude that neural mechanisms exist as early as in the primary visual cortex that are sensitive to figure-ground segregation. © 2000 Elsevier Science Ltd. All rights reserved.

Keywords: Functional magnetic resonance imaging; Primary visual cortex; Bold-response; Functional segmentation; Visual system

1. Introduction

Functional magnetic resonance imaging (fMRI), first described by Ogawa, Lee, Kay and Tank (1990a) and Ogawa, Lee, Nayak and Glynn (1990b), can indirectly visualise changes in neuronal activity. The visualisation is based on the fact that increased neuronal activity induces an increased blood flow, leading to a replacement of deoxygenated blood with oxygenated blood (Turner, Le Bihan, Moonen, Despres & Frank, 1991). The resulting changes in magnetic properties locally modulate the magnitude of the fMRI signal. Usually, the changes are small, around 1–3% of total signal strength. Improvement of both fMRI signal and signal-to-noise-ratio can be achieved by increased field strength (Turner, Jezzard, Wen, Kwong, Le Bihan, Zeffiro et al., 1993; Thulborn, Chang, Shen & Voyvodic, 1997). First successful attempts to visualise the activity of the visual cortex by means of fMRI have been made with flashing checkerboard patterns (Blamire, Ogawa, Ugurbil, Rothman, McCarthey, Ellermann et al., 1992) or flashing LEDs (Kwong, Belliveau, Chesler, Goldberg, Weisskopf, Poncelet et al., 1992; Ogawa, Tank, Menon, Ellermann, Kim, Merkle et al., 1992), using a uniform dark field as a control condition.

In the present study, we used more complex stimuli to detect activation specific for figure-ground segregation and segmentation, which is an important first step for object recognition in natural environments. Bach and Meigen (1992, 1997) found components in the visual evoked potentials (VEP) associated with texture segregation. Lamme et al. localised texture segregation-related activity at the primary visual cortex for orientation contrast and motion (Lamme, van Dijk & Spekreijse, 1993a,b; Lamme, 1995), combining electrophysiological and neurophysiological methods. Extending this work, experiments performed in our group using an 128-channel EEG (Fahle, Quenzer & Braun, unpublished data) found a segregation-specific component of cortical activity localised over the occipital cortex.

The main purpose of this study is to test whether a similar component defined by an increase of neuronal activity specific for figure-ground segmentation is present in the fMRI signal. If the signal shows a related component, the spatial scale of resolution for localising this component could be greatly improved compared to the EEG-recordings. Moreover, such a coincidence would lend added plausibility to the results of both

---

* Corresponding author. Tel.: + 49-421-2189526; fax: + 49-421-2189525.

E-mail address: mfahle@uni-bremen.de (M. Fahle)

these methods. There are indications that such an activation is indeed present in the BOLD (Blood-Oxygen-Level-Dependence) response of the fMRI: Reppas, Niyogi, Dale, Sereno and Tootell (1997) describe a segregation-specific component for figure-ground segmentation based on motion signals, with a centre of activation over the primary visual cortex.

2. Material and methods

2.1. Subjects

Five normal healthy volunteers (three females and two males, aged between 24 and 28 years) participated in this study. Their visual acuity was normal or corrected-to-be normal, refraction was between emmetropic and moderately myopic. Since observation distance was only 19 cm, refraction was corrected accordingly either by removing the spectacles (in the myopic observers), or by adding convex lenses of appropriate focal length.

Head motion during the functional scans was calculated by using a 2D-method based on an algorithm described by Friston, Ahsburner, Frith, Poline, Heather and Frackowiak (1995). The algorithm served to calculate the amount of head-motion within each scanning session, and to discard sessions with large head-motion. No comparison of head-motion between sessions was performed an no motion correction applied. The algorithm was tested after implementation by processing

images with artificially generated movements and rotations. Virtually none of the recordings did show any need for motion correction, with motion amplitudes below the in-plane diameter of one voxel, see Fig. 1 as an example for a good scan. Only the scan of one subject in one condition had to be discarded due to head motion.

2.2. Stimuli

The stimuli consisted of a luminance- (black and white checks), colour- (near isoluminant green and red checks), or motion-defined checkerboard (square shaped clouds of dots moving up versus dots moving down). Near isoluminance was provided by adjusting the luminance of the red and green elements to have the same luminance as measured with a Minolta LS-110 luminance meter. The checkerboard condition alternated with a uniform condition at a frequency of 0.012 Hz. The uniform condition corresponded to one of the two types of checks presented in the checkerboard, e.g. a homogeneous motion of a very large cloud of dots or an all green field. For example, the colour-defined stimulus started with an all green field, followed by a red-green checkerboard. After this checkerboard, the second homogeneous condition appeared, consisting of an all red field. The cycle was finished with a green-red checkerboard. A stimulus cycle was completed after these four different stimulus presentations (see Fig. 2). Each of the conditions was presented for 42.9 s, with no breaks between stimulus changes. As
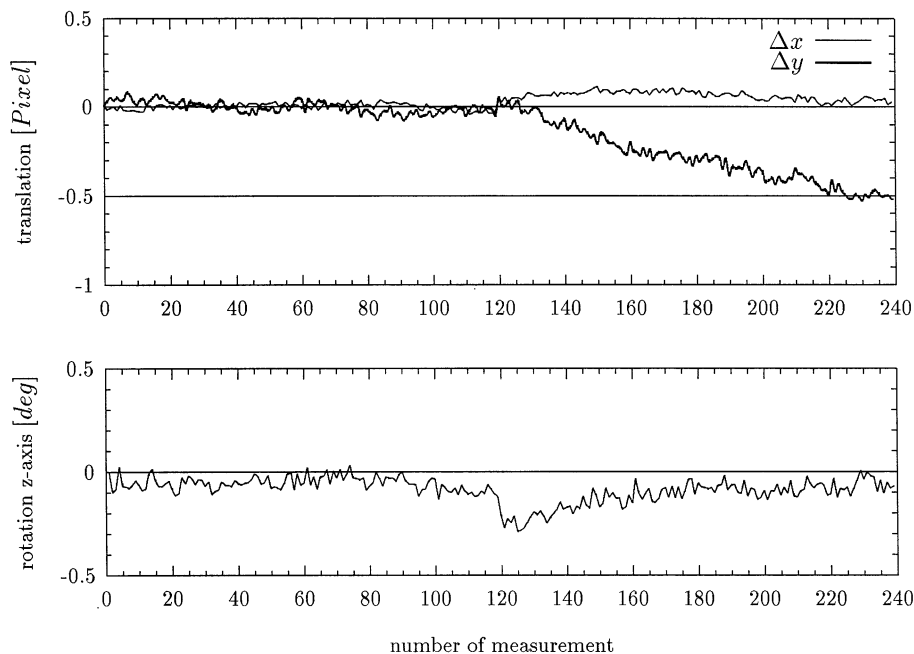

Fig. 1. Head motion during a scan session of subject JB. The graph displays the time course over 240 images (two stimuli, 120 images per stimulus).
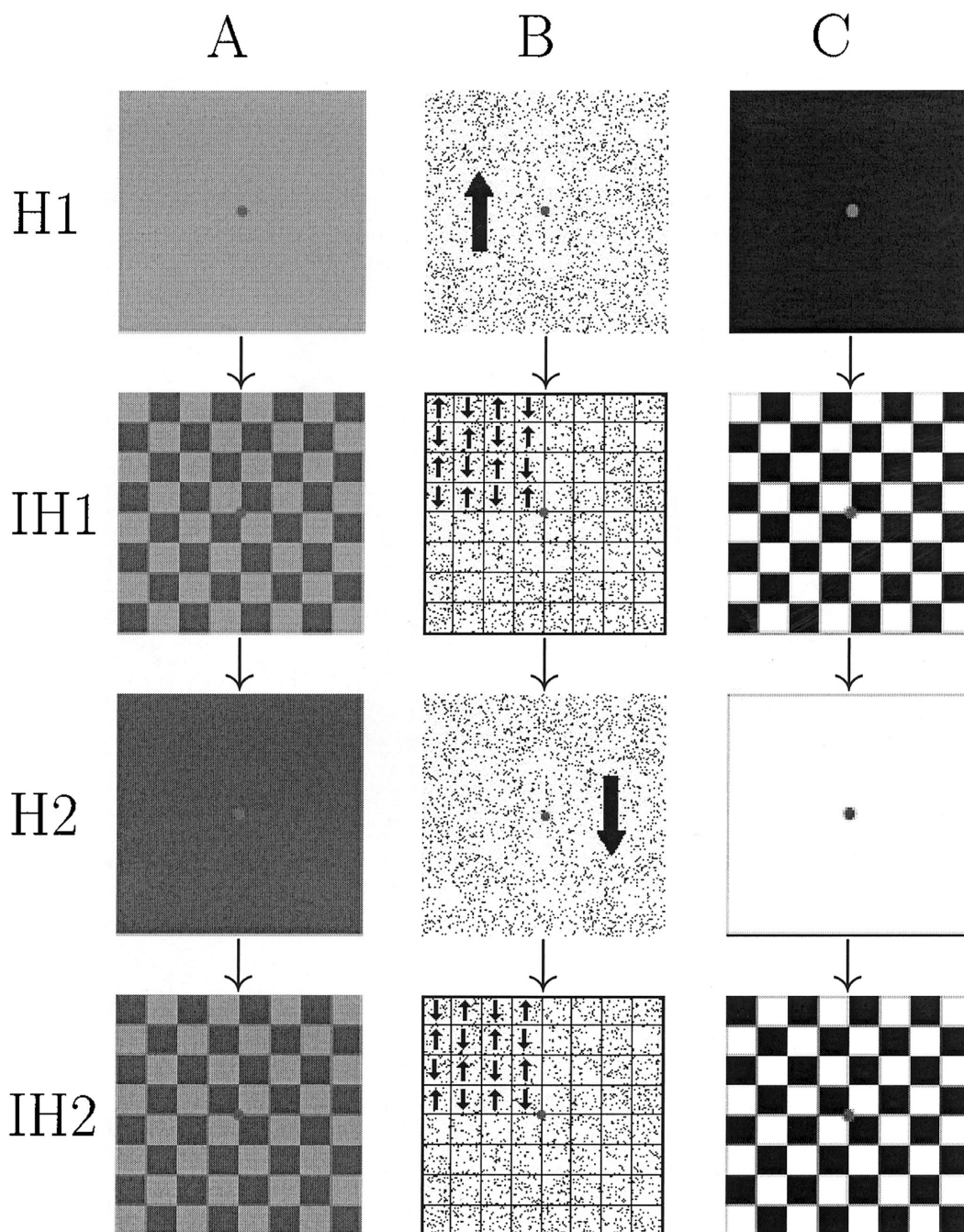
Fig. 2. Schematic representation of the stimuli used. The rows contain the subcycles of each type of stimulus. Every subcycle is presented from top to bottom for a duration of 42.9 s. (A) Colour-defined checkerboard (lighter grey indicates red, darker grey indicates green). (B) Motion-defined checkerboard. This stimulus starts with homogeneous motion upwards (H1), followed by a 'checkerboard motion' (IH1, see arrows). In H2 and IH2 the direction of motion is reversed. (C) Luminance-defined checkerboard.

a result, one cycle lasted 4×42.9 s $= 171.6$ s. Each cycle was repeated six times, so the presentation of one stimulus type lasted 6×171.6 s $= 17{:}09.6$ min. The stimulus subtended over a square area of about 25° of the visual field, corresponding, at the viewing distance of 19 cm, to an image size of 8.3×8.3 cm. The composition of our stimuli was similar to the one described by Bach and Meigen (1992, 1997), Lamme et al. (1993a,b) and Lamme (1995).

In addition, one subject (BZ) was scanned with the luminance stimulus flickered at 4 Hz to test whether or not the so-called segregation-specific activation may be caused by eye movements which might produce some form of a flicker- or motion-like stimulation at the borders between checks.

Stimuli were projected by means of a video projector (Sharp, model XG 3800E, with a lens of 300 mm focal length and an additional field lens) into the bore of the magnet on a small perspex screen. Subjects saw the screen through a mirror. Both mirror and screen were mounted on the headcoil.

2.3. Data acquisition

Subjects were scanned in a Siemens Vision 1.5 tesla system. We used 12 slices parallel to the calcarine sulcus for the T_1-weighted anatomical images, with an inter-slice gap of 1.25 mm, a slice thickness of 5.0 mm and an in-plane resolution of 0.95×0.95 mm. After anatomical images, functional images were collected using a T_2^*-weighted Echo-Planar-Imaging(EPI)-pulse-sequence (flip angle $= 90°$, TE $= 54.0$ ms for the motion- and luminance-defined checkerboard, TE $= 66.0$ ms for the colour-defined checkerboard). The in-plane resolution was 1.9×1.9 mm. During one stimulus presentation of 42.9 s five functional images were recorded. A full stimulus cycle was complete after presentation of four
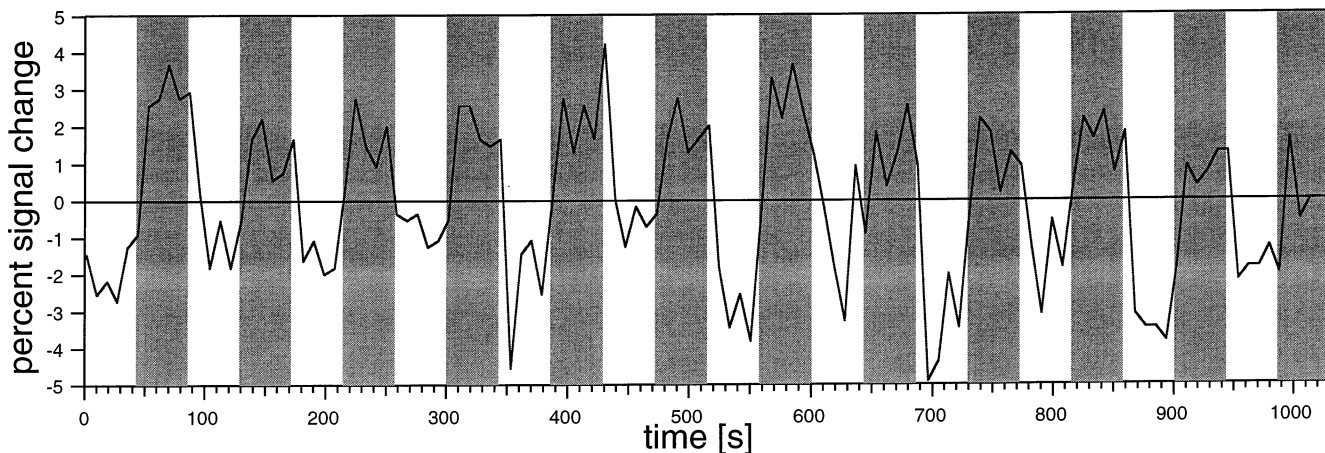

Fig. 3. Mean of the fMRI-signal from all pixels classified as active (slice 6 of subject JB, luminance-defined checkerboard). The gray bars mark the 'on'-periods of the stimulus (column C: IH1 and IH2 in Fig. 2).
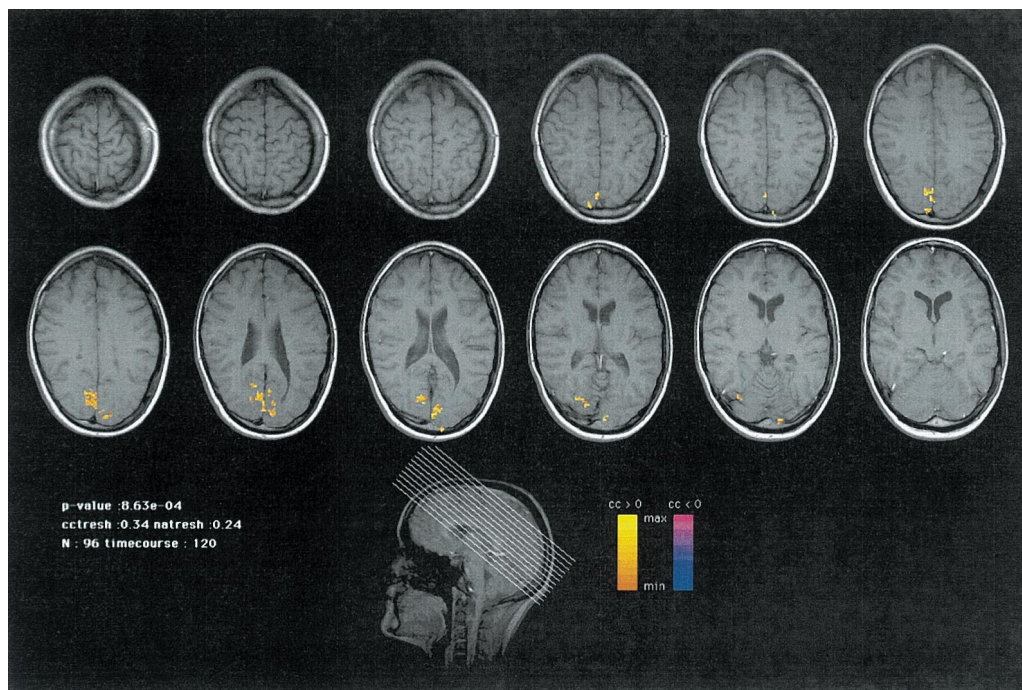

Fig. 4. Subject BZ, difference of the bold response between a luminance-defined checkerboard and a homogeneous stimulus. The activated pixels are colour coded, yellow for the amplitude maximum and red for the minimum in the respective slice. Negative correlation is marked in the same way from blue to pink. There is a bilateral activation in the occipital lobes, representing areas V1 and V2. Moderate right/left differences are explained by scull and ventricular asymmetries.
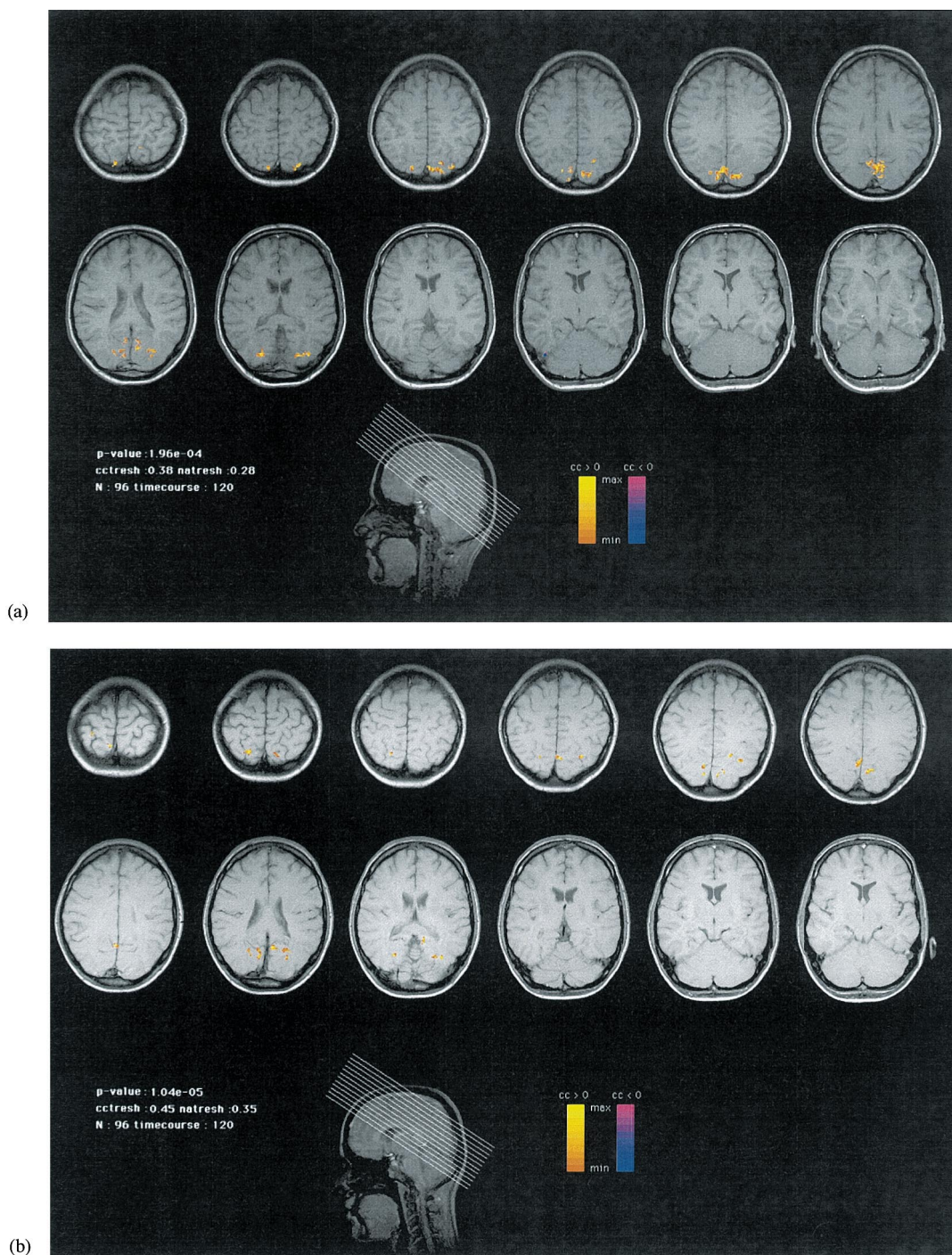
Fig. 5. (a) Subject JB, segmentation-specific components for the luminance-defined checkerboard. We find an activation pattern similar to Fig. 4, i.e. for observer BZ, but more symmetrical. (b) Subject JB, segmentation-specific components for the colour-defined checkerboard. Activation is similar to (a), i.e. for luminance-defined checkerboards. (c) Subject JB, segmentation-specific components for the motion-defined checkerboard. Activation especially in V1, with smaller components in V2 and V5.

different stimuli (see Fig. 2). Each stimulus cycle was repeated six times, resulting in $N = 5 \times 4 \times 6 = 120$ images for each slice during one functional scan. The presentation of the three types of stimuli was completed in two scanning sessions for each subject.

2.4. Image processing

All calculations were performed on Macintosh computers, with software developed in our laboratory. For further analysis, the first functional image after each

transition between stimuli was discarded because of the lag of the hemodynamic response, resulting in $N = 96$ images left for further processing. All images were inspected visually. If they contained artefacts, images were omitted from analysis. The time course vector for each pixel was correlated with an idealised box car vector using a method described by Bandettini and co-workers (1993). The box car vector was 'off' during the homogeneous (H) condition and 'on' during the checkerboard (IH) condition. Threshold values (cc_{tresh} in Figs. 4–7) were chosen to display the activation peak accurately. Due to different signal-to-noise ratios between subjects and between stimuli, it was not possible to chose the same threshold values for all experiments. To give information about the significance level of the chosen threshold values, P-values were computed (Bandettini, Jesmanowicz, Wong & Hyde, 1993). The evaluated activation was superimposed on the anatomical scans. Visual areas were localised according to gross anatomical landmarks and according to Talairach coordinates (see Talairach & Tournoux, 1988).

3. Results

The mean time course of an averaged signal from pixels classified as active is shown in Fig. 3. The signal change of the fMRI closely follows the changes in visual stimulation between homogenous fields (white) and checkerboards (dark), with no clear difference between the two types of checkerboards on one hand and the two types of homogenous fields on the other hand. Better correlation between stimulus and signal leads to higher correlation factors (as shown in Figs. 4–7, and to higher P-values, while looser correlations between stimulus and signal lead to lower correlation factors, hence no activation in Figs. 4–7). There was a bilateral activation of V1 with a smaller contribution of V2 in all subjects and for all stimuli (see Figs. 4–7). The Talairach main co-ordinates (Talairach & Tournoux, 1988) of the activated areas are shown in Table 1, for all subjects and all stimuli.

The colour- and luminance-defined checkerboard yielded stronger activation than the motion-defined stimuli did. For the checkerboards defined by motion, one of the segmentation-specific activations laid clearly outside of V1/V2 in three subjects (TH, GS, JB), namely in an area of the temporal cortex possibly corresponding to the human analogue of V5 (MT/MST; see Fig. 6 and Table 1). The stationary stimuli never activated an area which could be taken for V5. Subject BZ showed no significant difference between flickered and stationary luminance-defined stimuli (see Section 2.2).

4. Discussion

It has to be pointed out that the stimulation used in our experiments is of a rather subtle kind. Stimuli usually employed for fMRI studies consist of moving dots, or appearance and disappearance of luminous or
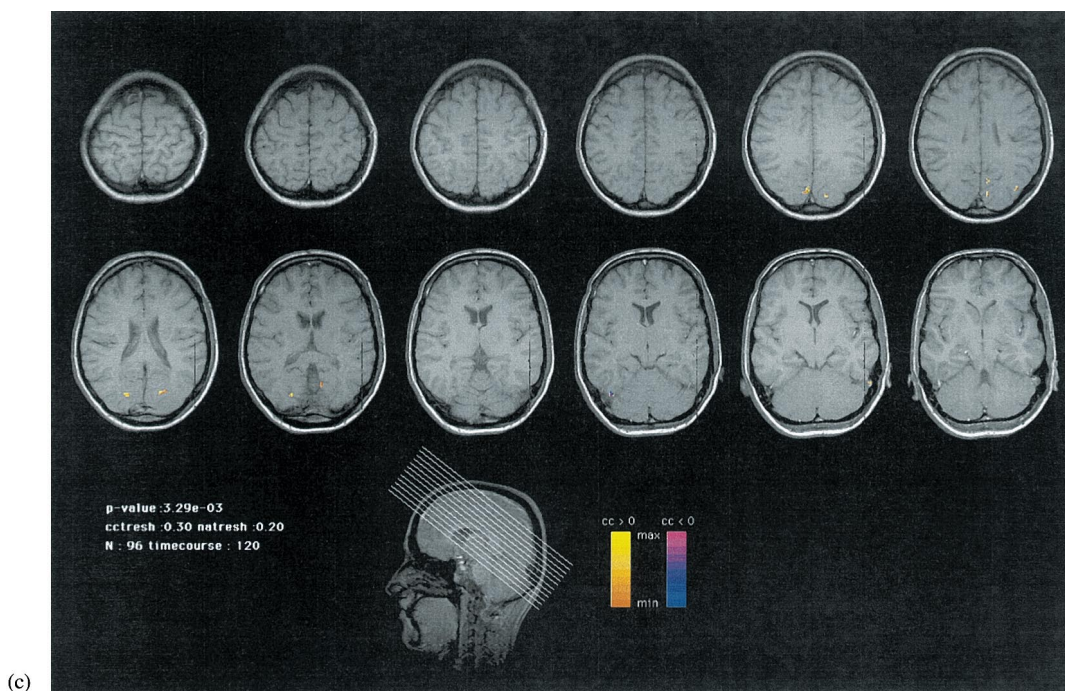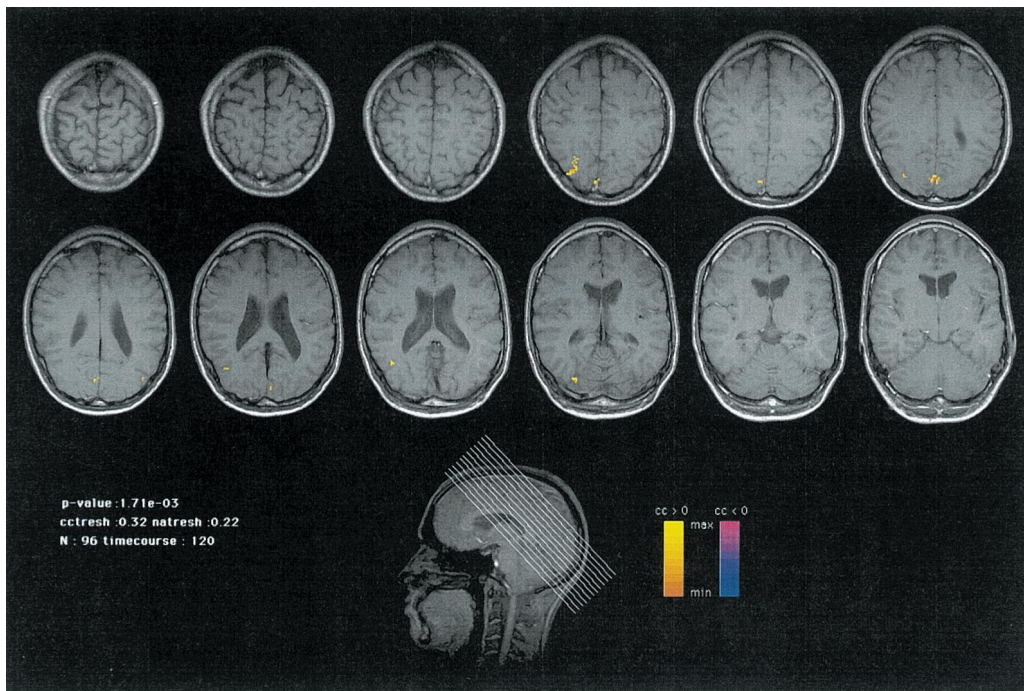

Fig. 5. (*Continued*)

Fig. 6
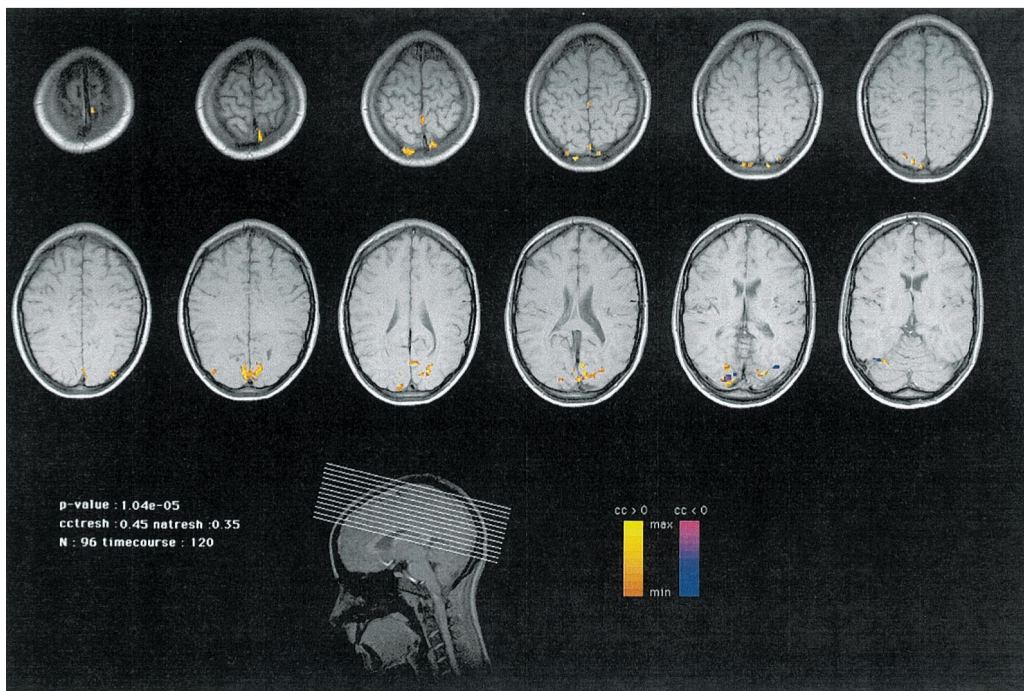
Fig. 7

Fig. 6. Subject TH, segmentation-specific components for the motion-defined checkerboard. The small activated area in the right occipito-parietotemporal cortex (left side of figure, according to neuroradiological convention) is supposed to represent the human homologue of area V5 (MT). Occipitally, there are strictly paramedian activations corresponding to V1.

Fig. 7. Subject AW, segmentation-specific components for the colour-defined checkerboard. Bilateral V1 and V2 activations.

Table 1
Talairach main co-ordinates of activated areas for all subjects and all stimuli

Paradigm	Subject	Activity (R/L) Talairach main coordinates)	P value[a]	Interpretation (R/L)
Luminance	JB	aH10/aH10	2.0×10^{-4}	V1/V2
		BH11/bH11		V2/V2
		AJ9/aj9		V2/V2
	TH	aJ10/aJ10	1.2×10^{-3}	V1/V1
		aJ9/aJ9		V2/V2
		Bg10/–		Vasc. Artefact
		–/bH11		–/V2
	GS	Ah9/Ah9	3.4×10^{-3}	V1/V1
	BZ	AH9/aH9	8.6×10^{-4}	V1/V2
		aH11/aH11		V2/V2
		aJ9/–		V2/–
Luminance flickered (4 Hz)	BZ	Ah9/Aj10	2.9×10^{-4}	V1/V1
		Aj9/Aj9		V2/V2
		Ah10/Ah10		V2/V2
Colour	JB	Ah10/Ah10	2.9×10^{-4}	V1/V1
		Bh11/Bh11		V2/V2
		Aj9/Aj9		V2/V2
	GS	Ah9/Ah9	1.0×10^{-5}	V1/V1
	AW	Ah9/Ah9	1.0×10^{-5}	V2/V2
		Aj9/Aj9		V2/V2
Motion	JB	Ah10/Ah10	3.3×10^{-3}	V1/V1
		Bh10/Bh10		V2/V2
		–/cH10		–/V5
	TH	AH9/aH9	1.7×10^{-3}	V1/V1
		Cg9/–		V5/–
		BH8/–		Not interpretable
	GS	aH9/aH9	3.3×10^{-3}	V1/V1
		BH9/bH9		V2/V2
		AH11/aH11		V2/V2
		Dg9/–		V5/–
	AW	aJ9/aJ9	3.3×10^{-3}	V1/V1
		AJ11/aJ11		V2/V2
		AJ9/–		V2/–[b]
	BZ	aH9/aH9	3.3×10^{-3}	V1/V1

[a] The P-values give information about the significance of the activations.
[b] Same main coordinates, but separate centers of activity.

coloured stimuli. The stimuli used in our experiments are much weaker in comparison since the two conditions that are compared and whose activations are correlated with each other both contain exactly the same elementary stimuli, just arranged in different ways. For example in the motion stimuli, the homogeneous conditions contain the same number and density of dots, moving at identical speeds as in the checkerboard conditions, so the only difference is the segmentation of the checks during presentation of the checkerboard. Therefore, we are able to demonstrate segmentation-specific activation, i.e. activation NOT due to the individual stimulus elements but to the fact that these elements differ along the borders of the checks.

The segmentation-specific activation could in principle be an artefact caused by a kind of flicker-response: eye movements have a much smaller effect on stimulation for homogeneous stimuli, where edges are present only in the peripheral visual field, than for segmented stimuli where moving borders between the segments might lead to a kind of flicker-response for the detectors near the borders. A control experiment ruled out that the activation we found is generated in the case of luminance- or colour-defined checkerboards through this possible artefact: flickering the homogeneous stimuli, thus generating a flicker response in all detectors rather than in only those close to the borders yielded a much smaller activation than the segmentation of the stimulus did. The motion stimulus contains a possible flicker-artefact, too. At the motion-defined borders, pixels appear and disappear randomly, which is not the case in the homogeneous condition. However, the activation of V1 in our motion-related experiments must not have originated from this flicker-artefact: Lamme et al. (1993b) and Lamme (1995) found neurones in V1 responding to motion-defined figure-ground segmentation, even though the corresponding control condition

with homogeneously moving dots contained this possible flicker-artefact at the checker-borders, too.

Strictly speaking, we cannot be sure that the colour-defined stimulus did not activate luminance-sensitive mechanisms since our isoluminant stimulus might have contained residual luminance differences due to inter-individual differences regarding the exact point of isoluminance. In addition, small differences of the isoluminance point exist between the fovea and the periphery of the retina. Further experiments, varying luminance contrast, will have to show whether low levels of luminance will be able to evoke a segmentation-specific cortical bold response. If not, the activation we find with the colour-defined checkerboard must be specific for colour.

A somewhat surprising finding is that the segmentation-specific activation is present already on the level of the primary visual cortex where one would not expect extensive motion- or colour-processing. However, the results of this fMRI study are in good agreement with those from multi-channel EEG recording using exactly the same type of stimuli (Fahle, Quenzer & Braun, unpublished). There exist models proposing that texture segmentation can be performed in the primary visual cortex (Lee, 1995), and additionally in V2, and perhaps in V3 or V5 (Mesrobian & Skrzypek, 1995). Lamme (1995) found in V1 of the macaque monkey's cortex neurones showing a stronger response to elements belonging to a figure than to similar elements belonging to the background. The figure-ground discrimination was achieved by differences in motion and orientation of the elements. Similar results were obtained using colour and luminance as a segmentation cue (Zipser, Lamme & Schiller, 1996). Therefore it seems safe to conclude that figure-ground segmentation based on luminance-, colour- or motion-cues is achieved at least partly in the primary visual cortex, maybe under the influence of top-down or feedback signals.

In V1, the activations caused by the motion-defined checkerboard, though relatively weak in comparison to colour and luminance, are in good agreement with the results of Reppas et al. (1997). These authors found an activation of V1 by a motion-defined checkerboard. In contrast to our findings, they detected no activation of V5. In at least one of our subjects, V5 is clearly activated in both hemispheres, and in two others there is a faint activation. This difference in results may originate from the different stimulus designs. In the stimuli used by Reppas et al., motion direction reversed at 1.2 Hz. In our stimuli, the homogeneous motion of the whole random dot field for 42.9 s during the control condition perhaps led to a weaker stimulation of V5 than in the inhomogeneous condition, where both directions of motion were present at the same time.

Hence we conclude that already the primary visual cortex of humans is involved in figure-ground segmentation based on differences in luminance, colour, and motion direction.

Acknowledgements

References

Bach, M., & Meigen, T. (1992). Electrophysiological correlates of texture segregation in the human visual evoked potential. *Vision Research, 32*, 417–424.

Bach, M., & Meigen, T. (1997). Similar electrophysiological correlates of texture segregation induced by luminance, orientation, motion and stereo. *Vision Research, 37*, 1409–1414.

Bandettini, P. A., Jesmanowicz, A., Wong, E. C., & Hyde, J. S. (1993). Processing strategies for time-course data sets in functional MRI of the human brain. *Magnetic Resonance in Medicine, 30*, 161–173.

Blamire, A. M., Ogawa, S., Ugurbil, K., Rothman, D., McCarthey, G., Ellermann, J. M., Hyder, F., Rattner, Z., & Shulman, R. G. (1992). Dynamic mapping of the human visual cortex by high-speed magnetic resonance imaging. *Proceedings of the National Academy of Sciences USA, 89*, 11069–11073.

Friston, K. J., Ahsburner, J., Frith, C. D., Poline, J. B., Heather, J. D., & Frackowiak, R. S. J. (1995). Spatial registration and normalization of images. *Human Brain Mapping, 3*, 165–189.

Kwong, K. K., Belliveau, J. W., Chesler, D. A., Goldberg, I. E., Weisskopf, R. M., Poncelet, B. P., Kennedy, D. N., Hoppel, B. E., Cohen, M. S., Turner, R., Cheng, H.-O., Brady, T. J., & Rosen, B. R. (1992). Dynamic magnetic resonance imaging of human brain activity during primary sensory stimulation. *Proceedings of the National Academy of Sciences USA, 89*, 5675–5679.

Lamme, V. A. F. (1995). The neurophysiology of figure-ground segregation in primary visual cortex. *The Journal of Neuroscience, 15*, 1605–1615.

Lamme, V. A. F., van Dijk, B. W., & Spekreijse, H. (1993a). Organization of texture segregation processing in primate visual cortex. *Visual Neuroscience, 10*, 781–790.

Lamme, V. A. F., van Dijk, B. W., & Spekreijse, H. (1993b). Contour from motion processing occurs in primary visual cortex. *Nature, 363*, 541–543.

Lee, T. S. (1995). A bayesian framework for understanding texture segmentation in the primary visual cortex. *Vision Research, 35*, 2643–2657.

Mesrobian, M., & Skrzypek, J. (1995). Segmenting textures using cells with adaptive receptive fields. *Spatial Vision, 9*, 163–190.

Ogawa, S., Lee, T.-M., Kay, A. R., & Tank, D. W. (1990a). Brain magnetic resonance imaging with contrast dependent on blood oxygenation. *Proceedings of the National Academy of Sciences USA, 87*, 9868–9872.

Ogawa, S., Lee, T.-M., Nayak, A. S., & Glynn, P. (1990b). Oxygenation-sensitive contrast in magnetic resonance image of rodent brain at high magnetic fields. *Magnetic Resonance in Medicine, 14*, 68–78.

Ogawa, S., Tank, D. W., Menon, R., Ellermann, J. M., Kim, S.-G., Merkle, H., & Ugurbil, K. (1992). Intrinsic signal changes accompanying sensory stimulation: functional brain mapping with magnetic resonance imaging. *Proceedings of the National Academy of Sciences USA*, *89*, 5951–5955.

Reppas, J. B., Niyogi, S., Dale, A. M., Sereno, M. I., & Tootell, R. B. H. (1997). Representation of motion boundaries in retinotopic human visual cortical areas. *Nature* (*London*), *388*, 175–179.

Talairach, J., & Tournoux, P. (1988). *Co-planar stereotaxic atlas of the human brain*. New York: Thieme Medical Publishers.

Thulborn, K. R., Chang, S. Y., Shen, G. X., & Voyvodic, J. T. (1997). High resolution echo-planar fMRI of human visual cor-tex at 3.0 tesla. *NMR in Biomedicine*, *10*, 183–190.

Turner, R., Le Bihan, D., Moonen, C. T. W., Despres, D., & Frank, J. (1991). Echo planar time course MRI of cat brain oxygenation changes. *Magnetic Resonance in Medicine*, *22*, 159–166.

Turner, R., Jezzard, P., Wen, H., Kwong, K. K., Le Bihan, D., Zeffiro, T., & Balaban, R. S. (1993). Functional mapping of the human visual cortex at 4 and 1.5 tesla using deoxygenation contrast EPI. *Magnetic Resonance in Medicine*, *29*, 277–279.

Zipser, K., Lamme, V. A. F., & Schiller, P. H. (1996). Contextual modulation in primary visual cortex. *The Journal of Neuro-science*, *16*, 7376–7389.